

Supplementary Information

Synergistic photocatalysis-Fenton reactions for selective conversion of methane to methanol at room temperature

Yi Zeng,^{a,#} Hang Chen Liu,^{a,#} Jing Sheng Wang,^a Xing Yang Wu^{a,b} and Song Ling Wang,^{a,b,*}

Experimental procedures

Materials

The commercial TiO₂ (P25), Fe₂O₃, NiO, CuO, ZnO and WO₃ catalysts are supplied by Macklin. FeCl₂·4H₂O was purchased from Macklin. H₂O₂ (30%) was supplied from Shanghai Lingfeng Chemical Reagent Co., Ltd. CH₄ (>99.99%) was supplied by Air Liquide. All of the chemicals above were used as received without further purification.

Characterizations

The crystal structure of the samples were measured by X-ray diffraction (XRD, SHIMADZU XRD-6100) with Cu K α radiation ($\lambda=1.54 \text{ \AA}$) in the 2θ range from 10° to 80°. The data was recorded at a scan rate of 5° / min. The morphology of TiO₂ was observed by transmission electron microscopy (TEM, FEI Tecnai G2 F20). Electron spin resonance (ESR) spectra of radical spin-trapped by 5,5-dimethyl-1-pyrroline N-

oxide (DMPO) were measured by a spectrometer (Bruker A300). In a typical measurement, 20 mg catalyst was dispersed in 20 ml deionized water. Then 2 ml 0.01M FeCl₂ solution was added in the above suspension, followed by stirring for 5 min. After that, 200 μl H₂O₂ was added in the suspension. 5,5-dimethyl-1-pyrroline N-oxide (DMPO) was used as the trapping reagent for both hydroxyl radicals (•OH) and superoxide radicals (•O₂⁻) detection. The ESR signals were collected after irradiation for 5 min (a xenon lamp with AM 1.5G filter was used as solar light source).

Conversion of methane

The Photocatalysis-Fenton reaction for conversion of methane was carried out in an autoclave of 130 ml volume equipped with a quartz window. A 300 W Xenon lamp (PLS-SXE 300, Perfect light) with AM 1.5G filter was used to provide solar light source. In a typical experiment, 20 mg catalyst were dispersed in 20 ml deionized water to form a suspension. Then, 2 ml FeCl₂ (0.01 M) solution was added into the above suspension, followed by stirring for 5 min. Subsequently, 200 μl H₂O₂ (30%) was added to the suspension (In these experiments of controlling H₂O₂ / Fe²⁺ ratios, the H₂O₂ dosages varied according to Fe²⁺ concentration). Thereafter, the above suspension was placed into the reactor (see Figure S1). Then, the reactor was purged with methane for several times to replace initial air. After that, 3 MPa methane was injected into the reactor. The Photocatalysis-Fenton reaction was then carried out under solar light irradiation and the temperature of the suspension was maintained at 30 °C.

After reaction for 1 h, the reactor was cooled in an ice bath for 1h. Subsequently, the gas in the reactor was injected into a gas chromatography to detect CO₂ and CO. Nevertheless, no CO₂ or CO were detected by the gas chromatography (KE CHUANG, GC 2002) equipped with two flame ionization detectors (FID1 and FID2) and one thermal conductivity detector (TCD). FID1 and TCD were connected to a TDX-01 column (2m × 3mm). The FID2 was connected to a GDX-502 column (4m × 3mm). The suspension in the reactor was then filtered and collected. The products (CH₃OH, CH₃CHO) in the solution collected from the suspension were analyzed with the gas chromatography mentioned above. Formic acid (HCOOH) in the solution was analyzed with a high performance liquid chromatography (SHIMADZU, Essentia CTO-16) equipped with a RSpak KC-811 6E column (Shodex) using 0.1% H₃PO₄ solution as mobile phase.

Selectivity and conversion rate calculation

The selectivity of methanol is calculated by the following equation:

The selectivity of methanol is calculated by the following equation:

$$\text{Selectivity (\%)} = \frac{N(\text{CH}_3\text{OH})}{N(\text{HCOOH}) + N(\text{CH}_3\text{OH}) + N(\text{CH}_3\text{CHO})} \times 100\%$$

$$\text{Conversion rate (\%)} \text{ of methane} = \frac{\text{moles of CH}_4 \text{ consumed}}{\text{moles of initial CH}_4} \times 100\%$$

Here, mole of CH₄ consumed = N (HCOOH) + N (CH₃OH) + 2N (CH₃CHO)”

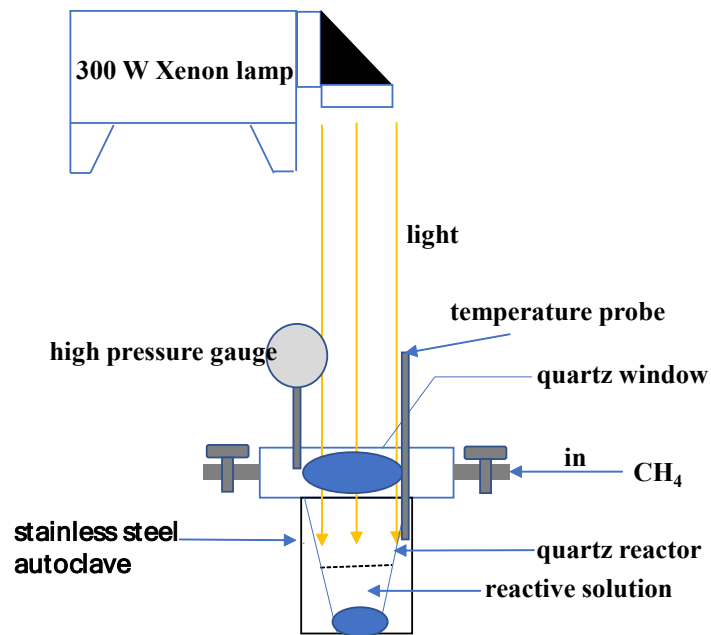


Fig. S1. Schematic reactor of conversion of methane.

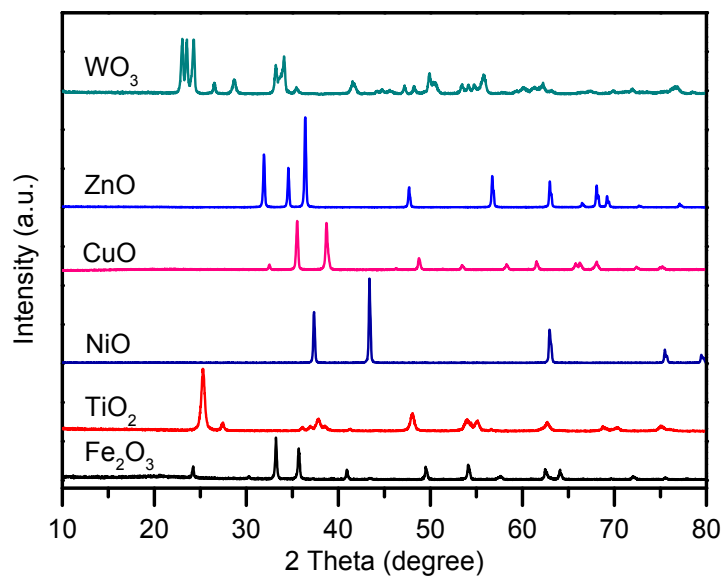


Fig. S2. XRD patterns of different catalysts.

Table S1. Conversion rates of methane in different PCFR, PCR, PFR, and FR processes.

Reactions	Products ($\mu\text{mol g}^{-1} \text{h}^{-1}$)			Selectivity (%)	Conversion rates (%)
	HCOOH	CH ₃ OH	CH ₃ CHO	CH ₃ OH	CH ₄
PCFR	34	471	53	84	0.39
PCR	64	64	0	50	0.08
PFR	0	165	59	74	0.15
FR	0	39	26	60	0.06

Table S2. Conversion rates of methane with different metal oxide semiconductor catalysts.

Catalysts	Products ($\mu\text{mol g}^{-1} \text{h}^{-1}$)			Selectivity (%)	Conversion rates (%)
	HCOOH	CH ₃ OH	CH ₃ CHO	CH ₃ OH	CH ₄
Fe ₂ O ₃	101	71	30	35	0.15
TiO ₂	34	471	53	84	0.39
NiO	300	52	32	14	0.27
CuO	454	151	38	23	0.43
ZnO	0	0	38	0	0.05
WO ₃	871	350	92	27	0.89

Table S3. Comparison of conversion of methane to methanol in different reactive processes over various catalyst reported.

Catalysts	Methods	Temperature and pressure	Generation rates of CH ₃ OH ($\mu\text{mol g}^{-1} \text{h}^{-1}$)	Selectivity of CH ₃ OH (%)	Ref.
La/WO ₃	^[a] PCR: mercury lamp, UVC-visible light	55 °C, 0.1MPa	32	47	1
WO ₃	PCR: mercury lamp, UVC-visible light	55 °C, 0.1MPa	55.5	38	2
BiVO ₄ /V ₂ O ₅	PCR: 450 W Hg lamp, UVC-visible light	70 °C, 0.1MPa	10.7	29.5	3
g-C ₃ N ₄ @Cs _{0.33} WO ₃	PCR: 300 W Xe lamp,	25 °C, 0.1MPa	4.38	51.5	4
BiVO ₄	PCR: 450 W mercury lamp,UVC-visible ligh	25 °C, 0.1MPa	21	50	5
BiVO ₄	PCR: 350 W Xe arc lamp, AM 1.5	65 °C, 0.1MPa	134	85	6
FeOOH/WO ₃	PCR: 300 W Xe lamp, visible light	25 °C, 0.1MPa	211	91	7
Cu/MOR	^[b] TDR: high temperature	200 °C, 0.7MPa	0.204mol/ Cu (mol)	97	8
Cu-ZSM-5	TDR: high temperature	200 °C, 0.1MPa	13	/	9, 10
TiO ₂	^[c] PCFR: 300 W Xe lamp, AM 1.5	30 °C, 3 MPa	471	83	this work

Abbreviations: ^[a]PCR, photocatalytic reaction; ^[b]TDR, thermodynamic reaction; ^[c]PCFR: photocatalysis-Fenton reaction

Table S4. Conversion rates of methane with different H₂O₂/Fe²⁺ ratios.

Ratios of H ₂ O ₂ /Fe ²⁺	Products ($\mu\text{mol g}^{-1} \text{h}^{-1}$)			Selectivity (%)	Conversion rates (%)
	HCOOH	CH ₃ OH	CH ₃ CHO	CH ₃ OH	CH ₄
0	0	0	0	0	0
10	0	162	0	100	0.10
20	34	471	53	84	0.39
50	53	325	180	58	0.47
120	179	294	189	44	0.48

References:

1. K. Villa, S. Murcia-López, J. R. Morante and T. Andreu, *Appl Catal B*, 2016, **187**, 30-36.
2. K. Villa, S. Murcia-López, T. Andreu and J. R. Morante, *Appl Catal B*, 2015, **163**, 150-155.
3. S. Murcia-López, M. C. Bacariza, K. Villa, J. M. Lopes, C. Henriques, J. R. Morante and T. Andreu, *ACS Catal*, 2017, **7**, 2878-2885.
4. Y. Li, J. Li, G. Zhang, K. Wang and X. Wu, *ACS Sustainable Chem. Eng*, 2019, **7**, 4382-4389.
5. S. Murcia-López, K. Villa, T. Andreu and J. R. Morante, *ACS Catal*, 2014, **4**, 3013-3019
6. Zhu W, Shen M, Fan G, *ACS Appl. Nano Mater.* 2018, 1, 6683–6691
7. J. Yang, J. Hao, J. Wei, J. Dai and Y. Li, *Fuel*, 2020, **266**.
8. V. L. Sushkevich, D. Palagin, M. Ranocchiari and J. A. van Bokhoven, *Science*, 2017, **356**, 523-527.
9. P. J. Smeets, M. H. Groothaert and R. A. Schoonheydt, *Catal Today*, 2005, **110**, 303-309.
10. A. A. Latimer, A. Kakekhani, A. R. Kulkarni and J. K. Nørskov, *ACS Catal.*, 2018, **8**, 6894-6907.